Geophysical Research Letters

Foraminifera Trace Anthropogenic CO_2 in the NW Atlantic by 1950

Stefanie Mellon[1], Markus Kienast[1], Christopher Algar[1], Peter de Menocal[2], Stephanie S. Kienast[1], Thomas M. Marchitto[3], Matthias Moros[4], and Helmuth Thomas[5]

[1]Department of Oceanography, Dalhousie University, Halifax, Nova Scotia, Canada, [2]Lamont-Doherty Earth Observatory, Palisades, NY, USA, [3]Department of Geological Science and Institute of Arctic and Alpine Research, University of Colorado Boulder, Boulder, CO, USA, [4]Leibniz Institute for Baltic Sea Research Warnemünde, Rostock, Germany, [5]Institute for Coastal Research, Helmholtz Center Geesthacht, Geesthacht, Germany

Abstract The Northwest Atlantic is a region of major climate change over the twentieth century, affected by the weakening of the Atlantic meridional overturning circulation. To assess whether the ability of this region to absorb anthropogenic CO_2 has been impacted by this change, we present the region's first long-term carbon isotope ($\delta^{13}C$) time series of fossil foraminifera spanning the past 4,000 years. These records reveal an unprecedented negative $\delta^{13}C$ excursion driven by anthropogenic CO_2 penetration into the surface ocean, the "Suess effect" signal. This signal (amplitude $-0.45‰$) emerges in 1950 CE $\pm$ 15 with a decrease rate of $0.009 \pm 0.001‰/yr$. This marine signal is $\sim$30% of the atmospheric Suess effect and emerges over a century later. Based on current estimates of the ratio of $\delta^{13}C_{DIC}$ change to dissolved inorganic carbon change and limited constraints on surface ocean residence times, we calculate a mean anthropogenic CO_2 uptake rate of $0.6 \pm 0.2\ \mu mol/(kg\ yr)$ from 1950 to 2005.

Plain Language Summary Since the industrial revolution, the burning of fossil fuels for human energy and transportation needs has caused an accumulation of carbon dioxide (CO_2) in the atmosphere. Over the same time period, nearly 30% of CO_2 emissions have been taken up by the ocean. This absorption is not uniform; therefore, understanding local CO_2 uptake rates is essential for assessing future ocean acidification risk. Our study investigates and presents the first long-term history of carbon for the Northwest Atlantic shelf region. The CO_2 emitted from fossil fuel burning has a distinct carbon isotope ratio compared to the preindustrial background level. Organisms called foraminifera incorporate the carbon isotope ratio of ocean carbon into their shells, which eventually sink to the seafloor where they are preserved in the sediments. For our analysis, we collected five sediment cores containing foraminifera from the NW Atlantic, resulting in carbon isotope records that span the last 4,000 years. We find evidence of fossil fuel-derived CO_2 in the NW Atlantic starting in 1950 and translate carbon isotope trends into estimates of fossil fuel CO_2 uptake rates by the surface ocean. Results from our study can be used to assess and predict future ocean acidification risk.

1. Introduction

The burning of fossil fuels has caused an accumulation of anthropogenic CO_2 in the atmosphere. The ocean is estimated to have taken up 152 ± 20 Pg of anthropogenic carbon, C_{ant}, from the beginning of the industrial revolution until 2007 (Gruber et al., 2019; Sabine et al., 2004), which is approximately 30% of the total emissions. Understanding the distribution of C_{ant} absorption within the ocean carbon sink is necessary for assessing future risks of climate change, such as ocean acidification.

The northwestern North Atlantic (NW Atlantic) is an important region for deep water formation and is characterized as a major C_{ant} sink (Sabine et al., 2004). Recent studies have identified the NW Atlantic shelves as a region that experienced significant climate change over the twentieth century due to a weakening of the Atlantic meridional overturning circulation (AMOC) by 15%, which is unprecedented over the past millennium (Caesar et al., 2018; Gilbert et al., 2005; Rahmstorf et al., 2015; Thibodeau et al., 2018; Thornalley et al., 2018). Accompanying this weakening are significant changes to several oceanographic characteristics of the NW Atlantic shelf region including an increase in temperature (Gilbert et al., 2005; Keigwin & Pilskaln, 2015; Thornalley et al., 2018), a nutrient regime shift (Sherwood et al., 2011) and deoxygenation (Gilbert et al., 2005). However, the state of the carbon system in this region is much less understood.
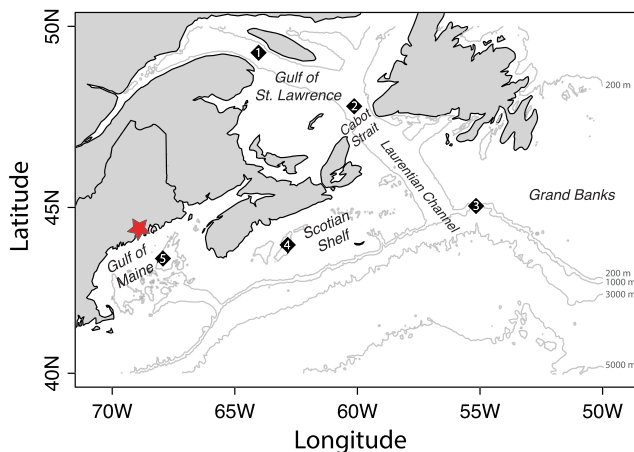
Figure 1. Locations of the core sites from this study denoted with black diamonds. 1, MSM46 MC4 from the GSL; 2, MSM46 MC2 from Cabot Strait; 3, KNR158 11MC13GGC from the Laurentian Slope; 4, OCE326 MC29 from Emerald Basin; 5, OCE400 MC44 from Jordan Basin. The location of the bivalve mollusk record from Schöne et al. (2011) is denoted by the red star.

Observations of decreasing pH in the bottom waters of the Lower St. Lawrence Estuary over the last 80 years suggest ocean acidification is a potential threat for the NW Atlantic shelves (Mucci et al., 2011). The deleterious effects of increased C_{ant} are likely exacerbated by rapidly changing local oceanographic conditions over NW Atlantic shelves (Gledhill et al., 2015) (see references above). This emphasizes the need to establish a historical record of the carbon cycle and C_{ant} in this region to distinguish natural variability from secular trends.

One method of tracking C_{ant} is by its isotopically light $\delta^{13}C$ signature. Ice cores and modern atmospheric measurements reveal an abrupt decrease in global $\delta^{13}C_{CO_2}$ of $-2.2‰$ since preindustrial times (Francey et al., 1999; Keeling et al., 2001; Rubino et al., 2013). This ubiquitous perturbation, first observed by Hans Suess in tree ring ^{14}C records, has been termed the "Suess effect" (Keeling, 1979). It is expected that the ^{13}C Suess effect (from here on referred to as the Suess effect) is detectable in $\delta^{13}C_{DIC}$ (dissolved inorganic carbon) of waters that are well ventilated with respect to the atmosphere and thus should be useful as a method of tracking C_{ant} penetration into the ocean (Gruber et al., 1999; Gruber & Keeling, 2001; Quay et al., 2007; Tans et al., 1993). However, few extensive, in situ time series measurements of $\delta^{13}C_{DIC}$ exist.

Most quantifications of the total Suess effect are based on a limited number of direct measurements of $\delta^{13}C_{DIC}$ (Quay et al., 2007) or back calculations using chlorofluorocarbons (Eide et al., 2017a; Körtzinger et al., 2003; Olsen & Ninnemann, 2010; Sonnerup et al., 1999). Paleoclimate proxies are valuable alternatives for reconstructing climate parameters further back in time (Swart et al., 2010). In particular, foraminifera are useful paleoproxies for $\delta^{13}C_{DIC}$ of the surface ocean because they precipitate calcium carbonate ($CaCO_3$) very close to isotopic equilibrium with the surrounding seawater (Ravelo & Hillaire-Marcel, 2007). Their shells are well preserved in the sediments under most open ocean conditions and thus can be collected from the seafloor for stable isotope analysis. A few studies have successfully reconstructed the Suess effect using this method in the Cariaco Basin (Black et al., 2011), the Arctic Ocean (Bauch et al., 2000), and the Gulf of Aqaba (Al-Rousan et al., 2004).

We present the first long-term time series of $\delta^{13}C$ for the NW Atlantic shelf region. We analyzed $\delta^{13}C$ records of foraminifera from five marine sediment cores spanning the Gulf of St. Lawrence (GSL), Laurentian Slope, Scotian Shelf, and Gulf of Maine (Figure 1). By applying this method to five different oceanographic regimes and four different species of foraminifera, we significantly reduce the regional and species-specific variability. We compare our findings to other quantifications of the Suess effect in the atmosphere and North Atlantic, as well as to the AMOC weakening over the twentieth century.

2. Methods

Sediment samples were collected from multicores (MC), a box core, and a gravity core (GC) at five locations (Figure 1). OCE400 44MC is a 53 cm long core collected from Jordan Basin (43°29′N, 67°53′W at 287 m depth) in August 2010, on board R/V *Knorr* (Keigwin & Pilskaln, 2015). OCE326 29MC is a 50 cm core collected from Emerald Basin (45°53′N, 62°48′W at 250 m depth) onboard R/V *Oceanus*, in July 1998 (Keigwin et al., 2003). The KNR158 11MC (59 cm) and 13GGC (300 cm) cores were collected on the Laurentian slope (11MC at 45°01′N, 55°13′W, 1,072 m depth; 13GGC at 45°01′N, 55°11′W, 1,035 m depth) in June 1998 on the R/V *Knorr* and are presented as a spliced record. The MSM46 MC2 (38 cm) and MC4 (30 cm) cores were collected in the Cabot Strait (47°50′N, 60°05′W, at 500 m depth) and Gulf of St. Lawrence (49°17′N, 63°59′W at 381 m), respectively, in August 2015, on board the R/V *Maria S. Merian*. Oxygen isotope records for the two OCE cores were previously published, but all $\delta^{13}C$ records are presented for the first time in this paper.

The cores were sampled at 1–5 cm intervals (supporting information Table S1). The sediment samples were washed with tap water through 63 μm sieves and subsequently dried at 60 °C. Planktic and benthic

foraminifera were picked according to specific size fractions (Table S1) and include the planktic species *N. pachyderma*, *G. bulloides*, and *N. incompta*, and the epibenthic species *C. lobatulus*. Stable carbon and oxygen isotopes were analyzed on all specified foraminifera samples and are expressed relative to the international standard, Vienna-PeeDee Belemnite according to equation (1). Foraminifera samples were analyzed on a variety of mass spectrometers, which are specified in Table S2 along with reported analytical precisions.

$$\delta 13C_{foram}(\text{‰}) = \frac{13C_{foram}/12C_{foram} - 13C_{VPDB}/12C_{VPDB}}{13C_{VPDB}/12C_{VPDB}} \times 1000 \qquad (1)$$

We assume that any potential impacts of genotype variation (Ravelo & Hillaire-Marcel, 2007), habitat migration during the life cycle (Hemleben & Bijma, 1994), and photosynthesis of algal symbionts (Bemis et al., 2000) are minimal because (a) foraminifera shells were picked at a constant size range throughout each core, (b) none of the species analyzed in this study have algal symbionts, and (c) there is no evidence or reason to expect systematic changes in genotype or habitat migration during the life cycle over the centennial to millennial time span sampled by the cores.

Additionally, we analyzed samples from MSM46 MC2 and MC4 for δ^{13}C of organic matter (δ^{13}C$_{org}$). Analysis was done on acidified samples (saturated with 10% HCl, dried at 50 °C, and transferred to silver capsules) with a microCube-Isoprime 100 instrument at Dalhousie University. The analytical error on δ^{13}C$_{org}$ of a blind standard was 0.11‰. δ^{13}C$_{org}$ data are presented in Tables S6 and S7.

Dating of the sediments was carried out using a combination of radiocarbon dates, ^{210}Pb measurements, and mercury (Hg) measurements based on sample and data availability. Age models were constructed in Bacon, an R-based Bayesian accumulation software that uses Markov Chain Monte Carlo iterations to estimate accumulation rates (Blaauw & Christen, 2011). Bacon's default input priors for accumulation rate and memory were used, 0.05 and 0.7 cm/yr, respectively. ^{14}C dates and ^{210}Pb data were used for OCE400 MC44 and OCE326 MC29 age-depth models. Hg data were used to construct the age models for MSM46 MC2 and MC4. KNR158 11MC and 13GGC were spliced together based on percent lithics and percent *N. pachyderma*. The ^{14}C from both these cores were used to construct the combined KNR158 11MC13GGC age model. Chronology data and resulting age-depth models are presented in Tables S3–S5 and Figure S2, respectively.

The ^{14}C dates were calibrated with the Marine13 calibration curve (Reimer et al., 2013) and a ΔR of 81 $\pm$ 76. The ΔR is based on the weighted average of 37 ΔR values from Atlantic Canada (McNeely et al., 2006). ^{210}Pb was measured indirectly via alpha counting of ^{210}Po (Sorgente et al., 1999), and the supported background ^{210}Po was determined using gamma spectrometry by measuring ^{226}Ra (Ghaleb, 2009). The Constant-Flux Constant-Supply model was used to determine the age-depth relationship (Appleby, 2002). Hg was used as a stratigraphic marker of modern sediments since Hg concentrations are influenced by anthropogenic pollution over the twentieth century (Engstrom & Swain, 1997; Leipe et al., 2013). Age models for MSM cores were constructed using Hg profiles and knowledge of local chlor-alkali plant operations and Hg emissions from the United States. The local Hg concentration increase began in the 1950s when the chlor-alkali plant in Saguenay Fjord started operations (Smith & Schafer, 1999). However, other Hg pollution sources in the United States started in the earlier twentieth century (1900–1940, Engstrom & Swain, 1997) and could potentially influence the Hg downcore profiles in our study region. Both of these Hg emission sources increased markedly in the 1960s, so the halfway point of this rapid increase was chosen as an age fix point (1960, Figure S1). This age point and a core top year of 2015 was input to Bacon to construct the age models (Figures S2a and S2b).

To constrain the Time of Emergence (ToE) and the magnitude and rate of change of any carbon isotope excursion (CIE), regression models with change point estimation were fit to the data using the R programming package "Segmented" (Muggeo, 2003). Results of this analysis are presented in Figure S3. For each δ^{13}C record, a two-piece regression was fit with time as the predictor variable and δ^{13}C as the response. In cases where a two-piece regression resulted in an insufficient fit to the data, a three-piece regression was used instead. If the most recent segment (or two most recent segments) had a negative slope, the trend was considered a CIE and the δ^{13}C decrease rate was defined by the slope of that segment. The magnitude of the CIE was determined as the difference between δ^{13}C at the change point and the modeled δ^{13}C
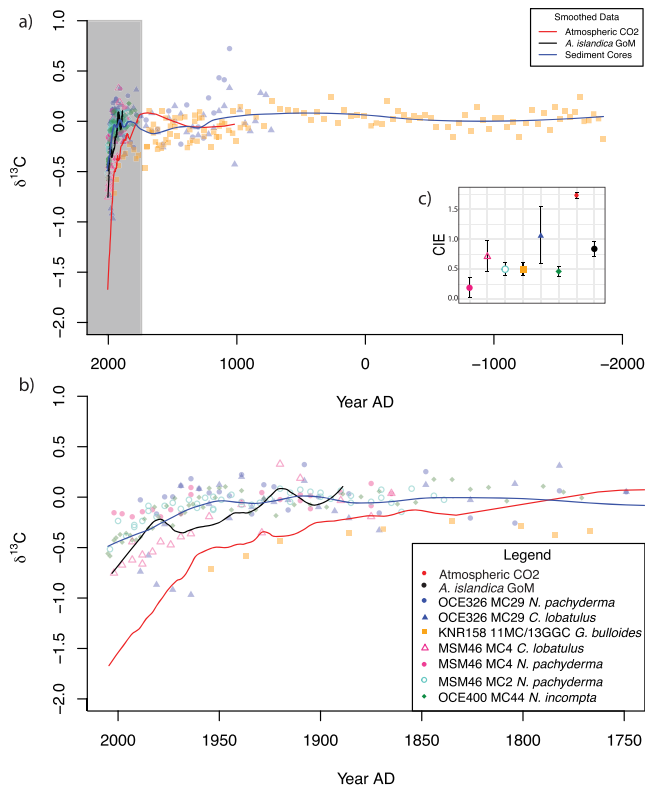
Figure 2. Stable carbon isotope anomalies of foraminifera over (a) the late Holocene and (b) the Anthropocene from NW Atlantic sediment cores (symbols—see legend). The smoothed blue curve is a Loess regression of all the foraminifera δ^{13}C data from this study. A Loess regression was also applied to δ^{13}C records from ice core and atmospheric CO_2 (red; Graven et al., 2017) and a long-lived bivalve *A. islandica* from the Gulf of Maine (black) (Schöne et al., 2011). Symbols representing δ^{13}C records from the same core are plotted with the same color, while those of the same species are plotted with the same shape (see legend). (a) From 2000 BCE to 2005 CE. (b) From 1750 to 2005 CE. (c) Magnitude of the carbon isotope excursion (CIE) for each record. Error bars represent the 1 sigma standard deviation.

value at the most recent sample age. In core MSM46 MC4 (see Figure S3d), where the change point did not seem to represent the preindustrial δ^{13}C value, it was determined by averaging the δ^{13}C values of all samples older than the CIE. In order to compare magnitudes of the CIE between cores, the CIEs were normalized by extrapolating their respective models to 2005 CE. That year was chosen because it is the mean age of the most recent sample collected in this study (MSM46 MC2, 0.5 cm). For better comparison with the foraminifera records, the piecewise regression method was also applied to the atmospheric $\delta^{13}C_{CO2}$ record from Graven et al. (2017) and marine bivalve δ^{13}C record from the Gulf of Maine (*A. islandica*; Schöne et al., 2011).

The uncertainties were quantified based on 1σ uncertainty in the piecewise regression models, displayed as both 95% confidence and prediction intervals. In addition, uncertainty in the timing of the change point was estimated by applying the piecewise regression to δ^{13}C records with depth (instead of time), and then converting the depth change point to age, using Bacon. Bacon computed the associated age and uncertainty for each given change point depth.

To calculate the average Suess effect for the region, we computed the weighted mean of the CIEs. The weighting was based on the 1σ uncertainty in the calculated magnitude of each CIE. For the average δ^{13}C decrease rate, we calculated the weighted mean of the slope of the piecewise regression postchange point using a weighting relative to the 1σ uncertainty in the slope. For the ToE determination, we calculated the weighted average of all the change points using a weighting system relative to the 1σ uncertainties of the age-depth and piecewise linear regression models. The calculation of all three of these parameters excludes the *N. pachyderma* record of core OCE326 MC29, which does not display the negative CIE.

An alternative method was also used to determine the Suess effect characteristics for the study region as a whole. Foraminifera species precipitate $CaCO_3$ at a small, near-constant isotopic offset from DIC; however, this offset differs between species. For a direct comparison of trends in the data, the foraminifera δ^{13}C records were, therefore, standardized by subtracting the preindustrial mean δ^{13}C. The piecewise linear regression analysis was applied to all of these standardized data to obtain magnitude, ToE, and δ^{13}C decrease rate of the regional Suess effect.

3. Results

The foraminiferal δ^{13}C records clearly reveal negative CIEs in the modern sections of the cores (Figures 2 and S3). There is minimal variability prior to the CIEs, indicating this event is unprecedented over the 150–4,000 years sampled by these cores (with the exception of Emerald Basin, core OCE326 MC29, *N. pachyderma*, Figure S3e). The observed CIEs range from -0.174 ± 0.164 to -0.757 ± 0.290‰ (Figure 2 and Table 1), with the weighted average for 2005 of 0.469 ± 0.053‰ (regional standardized record, 2005: 0.456 ± 0.084‰). Only one planktonic record out of the seven δ^{13}C records studied here does not exhibit a modern negative CIE (OCE326 MC29, *N. pachyderma*), but the epibenthic record from the same core does show a clear CIE (Figure S3f). The weighted mean of the ToE between all records (except OCE326 MC29 *N. pachyderma*) is 1950 CE $\pm$ 15 years (regional standardized record yields: 1957 $\pm$ 5 years). The weighted mean of the δ^{13}C decrease rate since the ToE is -0.00945 ± 0.00081‰/yr (regional standardized record yields: -0.009497‰/yr, $R^2 = 0.329$). Results of the piecewise regression models are presented in Figure S3. All CIE and δ^{13}C rate of change estimates are presented in Table 1, and cumulative uncertainties for the ToE from the age model and regression analysis are presented in Table S8. Signal to noise ratios ranged from 3.3 to 8.6 (Table S9).

Table 1
Summary Table of the Piecewise Linear Regressions for Each Core as Well as Graven et al.'s (2017) Atmospheric CO_2, Schöne et al.'s (2011) A. islandica, and the Standardized Data From All Cores

Core	Species	Change point (year, CE)	Adjusted R^2	Rate of change (‰/yr)	Observed CIE (‰)	2005 CIE (‰)
MSM46 MC4	*N. pachyderma*	1963 ± 41	0.463	-0.0006 ± 0.001 -0.0045 ± 0.0018	0.174 ± 0.164	0.187 ± 0.170
MSM46 MC4	*C. lobatulus*	1913 ± 75	0.801	0.005 ± 0.004 -0.0095 ± 0.0014	0.69 ± 0.257	0.718 ± 0.260
MSM46 MC2	*N. pachyderma*	1910 ± 73 1984 ± 4[a]	0.767	0.0008 ± 0.0007 -0.0021 ± 0.0007 -0.0166 ± 0.0033	0.486 ± 0.103	0.498 ± 0.111
KNR158 11MC/13GGC	*G. bulloides*	1505 ± 176	0.53	0 ± 0 -0.001 ± 0.0002	0.452 ± 0.099	0.502 ± 0.113
OCE326MC29	*N. pachyderma*	1261 ± 362	0.508	-0.0037 ± 0.0008 0.0002 ± 0.0001	-0.132 ± 0.22	-0.135 ± 0.221
OCE326 MC29	*C. lobatulus*	1950 ± 29	0.437	-0.0001 ± 0.0001 -0.0195 ± 0.0068	0.758 ± 0.29	1.068 ± 0.48
OCE400 MC44	*N. incompta*	1962 ± 23	0.808	-0.0006 ± 0.0003 -0.0108 ± 0.0014	0.459 ± 0.082	0.459 ± 0.082
Graven et al. (2017)	Ice, firn, CO_2	1805 ± 6[a] 1958 ± 1[a]	0.991	0.0002 ± 0.0001 -0.0038 ± 0.0001 -0.0247 ± 0.0003	1.997 ± 0.049	1.737 ± 0.047
All (2005)	All	1957 ± 5[a]	0.329	0 ± 0 -0.0095 ± 0.0015	0.456 ± 0.084	
Schöne et al., 2011	*A. islandica*	1920 ± 5[a] 1969 ± 2[a] 1980 ± 2[a]	0.771	0.0016 ± 0.0022 -0.0085 ± 0.0011 0.0198 ± 0.0104 -0.0255 ± 0.0032	0.788 ± 0.116	

Note. The change point error contains the 1σ uncertainties in both the piecewise linear regression and the age model (See Table S8 for breakdown). Observed CIEs, 2005 adjusted CIEs are presented with their respective 1σ errors.
[a]Only the piecewise linear regression uncertainty.

The average preindustrial $\delta^{13}C$ is $-0.02‰$ for *G. bulloides*, 0.64–0.91‰ for *N. pachyderma*, 0.51–0.67‰ *for C. lobatulus*, and 0.75‰ for *N. incompta*. The standardized $\delta^{13}C$ data from all cores are displayed as points on the anomaly plot in Figure 2, along with the smoothed $\delta^{13}C$ trend of atmospheric CO_2 (Graven et al., 2017) and the bivalve $\delta^{13}C$ record from the Gulf of Maine *(A. islandica, Schöne et al., 2011)*.

4. Discussion

Despite very different oceanographic settings, negative $\delta^{13}C$ excursions (CIEs) are seen in the top sections of the cores at all five locations and are unprecedented over the entire 150–4,000 years sampled by the cores (Figure 2a). Because these CIEs are observed in $\delta^{13}C$ records of four different foraminifera species with different sensitivities to environmental conditions, we deem the impact of slight disequilibria with the surrounding DIC pool caused, for example, by calcification temperature (Bemis et al., 2000), seawater pH (carbonate ion concentration) (Hesse et al., 2014; Spero et al., 1997), and foraminiferal diet (King & Howard, 2004) on our determinations of the Suess effect parameters to be minimal. This assertion is further supported by the $\delta^{13}C_{org}$ from both MSM46 cores, as the amplitudes of the negative CIEs are indistinguishable in these two independent archives (Figure 3).

The atmospheric CO_2 Suess effect is the main controlling factor on the Suess effect in the surface ocean DIC pool (Körtzinger et al., 2003; Quay et al., 1992). It takes approximately 10 years for these two reservoirs to reach isotopic equilibrium (Lynch-Stieglitz et al., 1995), suggesting that the surface ocean should track the atmosphere with minimal delay. The three-piece regression analysis of the historical $\delta^{13}C$ atmospheric CO_2 record of Graven et al. (2017) reveals a Suess effect of $-1.74 \pm 0.05‰$ for 2005. The ToE in the atmosphere is 1804, with a decrease rate of $-0.0038‰/yr$, which steepened substantially to $-0.025‰/yr$ after 1958. The foraminifera isotope records (CIE = $0.456 \pm 0.084‰$), therefore, express only ~30% of the atmospheric signal amplitude, and the foraminiferal ToE (1950 CE $\pm$ 15 years) lags by over a century, making it indistinguishable from the time the trend steepened in the atmosphere.
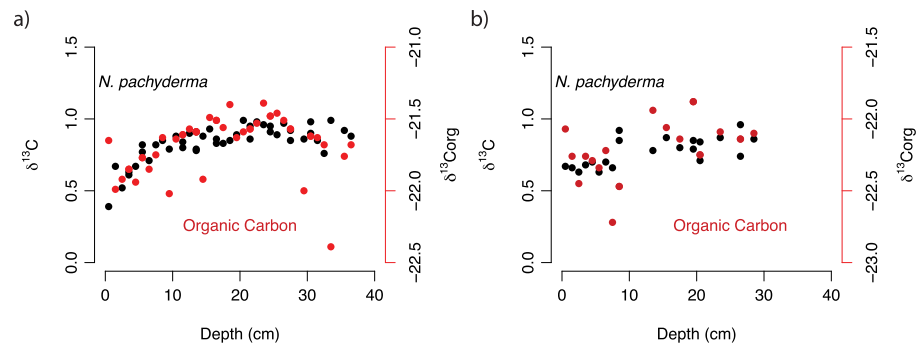
AGU
100
ADVANCING EARTH
AND SPACE SCIENCE

Geophysical Research Letters

10.1029/2019GL084965

Figure 3. δ^{13}C of organic carbon (red) and *Neogloboquadrina pachyderma* (black) time series results of cores (a) MSM46 MC2 and (b) MSM46 MC4.

What could explain this considerable lag between the atmosphere and the subsurface ocean? It may be due in part to isotopic disequilibrium between the surface ocean and atmosphere. Water masses may not remain at the surface for the 10 years necessary to reach equilibrium with the atmosphere, which means surface residence times are an important factor in the expression of the DIC Suess effect. Modeling studies suggest that the atmosphere to ocean ratio of the Suess effect has a global mean of 0.6–0.7 over the industrial period (Broecker & Peng, 1993), with a ratio closer to 1:1 only in recent decades (Eide et al., 2017a). By contrast, our results reveal a ratio closer to 0.3 for the continental shelf region of the NW Atlantic. Given the ~0.3‰ scatter in the δ^{13}C core measurements, it may not be possible to resolve the smaller-magnitude atmospheric δ^{13}C change between 1804 and 1958 because of the small signal-to-noise ratio.

The foraminiferal δ^{13}C decrease rate of -0.009 ± 0.001‰/yr reported here is consistently lower than open ocean estimates for the North Atlantic. Direct δ^{13}C measurements from transects taken in 1981 and 2003 in the subtropical northwest Atlantic (20–40°N) show a decrease rate of -0.025‰/yr (Quay et al., 2007), with lower rates in the tropics (-0.011 ± 0.003‰/yr) and subpolar region (-0.017 ± 0.005‰/yr). The reported global mean ranges from -0.015 to -0.018‰/yr (Gruber et al., 1999; Sonnerup et al., 1999) since the 1970s. A planktic foraminifera (*G. ruber*) record from a high-resolution, laminated sediment core in the Cariaco Basin shows a near tripling of the δ^{13}C decrease rate from -0.01‰/yr before 1950 to -0.025‰/yr at 2008 with an overall CIE of -0.75‰ (Black et al., 2011). Since there are no δ^{13}C data available from other subpolar coastal sites for direct comparison, it is difficult to establish whether the slower δ^{13}C rate of change is a regional anomaly or representative of coastal environments more generally.

Bioturbation is a possible mechanism to explain dampening of climate signals (Anderson, 2001; Charbit et al., 2002). This process homogenizes the upper layers of sediment, obscuring decadal changes in the paleo record, the exact time scale over which the Suess effect occurs. However, a diagenetic model describing depth profiles of ^{210}Pb, ^{13}C, and ^{12}C that includes a bioturbation depth to the global average of 10 cm (Boudreau, 1994) was applied to cores OCE326 MC29 and OCE400 MC44 (see Text S1 of supporting information) and confirmed that bioturbation is not a significant factor in the observed Suess effect signal at these sites. It is reasonable to assume this would apply at the other locations as well. This assertion is supported by a well-dated bivalve mollusk record from the Gulf of Maine (Schöne et al., 2011), which is not affected by bioturbation and also displays a relatively small Suess effect (-0.83‰ in 2005) and a delayed ToE (1920) in comparison to the atmosphere. The δ^{13}C decrease rate is -0.008‰/yr after 1920 and then steepens to -0.026‰/yr after a brief δ^{13}C increase between 1969 and 1980. The foraminifera track the initial decrease but not the pause or the steepening displayed by the mollusk record. Overall, however, the close agreement between the foraminifera and mollusk records suggests that the δ^{13}C signals displayed in the foraminifera are representative of the subsurface water DIC pool in the study region.

Assuming that our observations of the Suess effect from foraminiferal δ^{13}C are representative of the DIC pool, what could make this region different from other parts of the North Atlantic and the global ocean? Recent studies of the North Atlantic report anomalously weak AMOC over the twentieth century (Caesar et al., 2018; Rahmstorf et al., 2015; Thibodeau et al., 2018; Thornalley et al., 2018). As a result, there was a

change in the relative influence of water masses on the NW Atlantic shelf region. Observations suggest a decreased transport of colder, fresher, oxygen-rich water via the Labrador Current (Labrador Subarctic Slope Water) and an increased influence of warmer, saltier, nutrient-rich water from the subtropical gyre (Atlantic Temperate Slope Water). The resulting subsurface temperature increase (Gilbert et al., 2005; Thornalley et al., 2018), pH decrease (Mucci et al., 2011), oxygen depletion (Gilbert et al., 2005), and a nutrient regime shift (Sherwood et al., 2011) may influence air-sea CO_2 exchange rates, biological production, and advected DIC—which all affect $\delta^{13}C$ of DIC. It is difficult with the available data to tease apart the relative influence of these processes on $\delta^{13}C$ of DIC, but increased presence of the older, nutrient-rich Atlantic Temperate Slope Water (Mucci et al., 2011) may contribute to a later appearance and smaller magnitude of the Suess effect compared to other North Atlantic surface waters and the atmosphere.

5. Anthropogenic CO_2 Estimations

The regionally coherent negative $\delta^{13}C$ excursions attributed to the Suess effect allow for the estimation of C_{ant} penetration into the shelf region of the NW Atlantic from the ratio of $\delta^{13}C_{DIC}$ change to DIC change ($\Delta RC = \Delta\delta^{13}C/\Delta DIC$) (Heimann & Maier-Reimer, 1996). The global average ΔRC, based on a regressional relation of gridded data, is estimated to be $-0.013‰/(\mu mol/kg)$ (Eide et al., 2017b). However, observations suggest this value varies significantly from region to region and using the global average can lead to errors in the C_{ant} uptake rate by up to 50% (McNeil et al., 2001). This is because ΔRC depends on atmospheric exposure times of water masses before subduction (Eide et al., 2017b). No ΔRC values are available specifically for the coastal NW Atlantic, and therefore we use a back-of-the-envelope calculation to illustrate the general utility of foraminifera data for constraining C_{ant} fluxes using average North Atlantic ΔRC values.

Eide et al. (2017a) determined the mean ΔRC for the entire North Atlantic basin to be $-0.015 \pm 0.006‰/(\mu mol/kg)$. Using this mean North Atlantic ΔRC value and our finding of $\Delta\delta^{13}C = -0.009 \pm 0.001‰/yr$ yields a C_{ant} uptake rate of $0.6 \pm 0.2 \mu mol/(kg\ yr)$. Within our observational window (ToE 1950 $\pm$ 15 until 2005), $p CO_2$ has increased 1.4 ppm/yr. Given the C_{ant} uptake rate of $0.6 \mu mol/(kg\ yr)$ implied by our $\delta^{13}C$ records, this corresponds to a Revelle factor of 11–13, which agrees well with the value reported for the region (Thomas et al., 2007). For the open North Atlantic, Körtzinger et al. (2003) report an uptake rate of $1.2 \mu mol/(kg\ yr)$. The somewhat lower values suggested for our study area could be due to a higher Revelle factor in coastal and shelf regions (due to lower alkalinity). Alternatively, the somewhat lower uptake rates could be due to the "estuarine" circulation pattern on the Scotian Shelf and in the St. Lawrence, which also may serve to explain the above discussed CIE lag between the atmosphere and the subsurface waters.

For better comparison with global estimates of anthropogenic CO_2 flux (Gruber et al., 2019), and assuming an annual average mixed layer depth of 38.7 ± 32 m for the study region (Atlantic Canada Model; the high standard deviation in the mixed layer depth is due to the high seasonality in this region) (Brennan et al., 2016), we translate the C_{ant} uptake rate to a CO_2 flux of $0.024 \pm 0.021\ (mol\ C/m^2)/yr$.

In summary, we have established the first long-term $\delta^{13}C_{DIC}$ history integrated over the NW Atlantic shelf region. Our results clearly show the Suess effect (negative CIE) beginning in 1950 CE $\pm$ 15 with a magnitude of $-0.45‰$ and a near constant $\delta^{13}C$ decrease rate of $0.009 \pm 0.001‰/yr$. The CIE is unprecedented over the last 4,000 years. Importantly, the $\delta^{13}C$ rate of change observed in the foraminifera records is consistent with thermodynamic considerations (Revelle factor), thus providing a constraint for regional models that hindcast and forecast anthropogenic CO_2 changes in this coastal region. Furthermore, our records suggest that changes in ocean circulation can exert an important control on C_{ant} uptake.

References

Al-Rousan, S., Patzold, J., Al-Moghrabi, S., & Wefer, G. (2004). Invasion of anthropogenic CO_2 recorded in planktonic foraminifera from the northern Gulf of Aqaba. *International Journal of Earth Sciences*, *93*(6), 1066–1076. https://doi.org/10.1007/s00531-004-0433-4

Anderson, D. M. (2001). Attenuation of millennial-scale events by bioturbation in marine sediments. *Paleoceanography and Paleoclimatology*, *16*(4), 352–357.

Appleby, P. G. (2002). Chronostratigraphic techniques in recent sediments. In W. M. Last & J. P. Smol (Eds.), *Tracking environmental change using lake sediments*, *Developments in Paleoenvironmental Research* (Vol. 1, pp. 171–203). Dordrecht: Springer.

Bauch, D., Carstens, J., Wefer, G., & Thiede, J. (2000). The imprint of anthropogenic CO_2 in the Arctic Ocean: Evidence from planktic delta^{13}C data from watercolumn and sediment surfaces. *Deep-Sea Research Part II: Topical Studies in Oceanography*, *47*, 1791–1808. https://doi.org/10.1016/S0967-0645(00)00007-2

Bemis, B. E., Spero, H. J., Lea, D. W., & Bijma, J. (2000). Temperature influence on the carbon isotopic composition of *Globigerina bulloides* and *Orbulina universa* (planktonic foraminifera). *Marine Micropaleontology*, *38*(3–4), 213–228. https://doi.org/10.1016/S0377-8398(00)00006-2

Blaauw, M., & Christen, J. A. (2011). Flexible paleoclimate age-depth models using an autoregressive gamma process. *Bayesian Analysis*, *6*(3), 457–474. https://doi.org/10.1214/11-BA618

Black, D., Thunell, R., Wejnert, K., & Astor, Y. (2011). Carbon isotope composition of Caribbean Sea surface waters: Response to the uptake of anthropogenic CO_2. *Geophysical Research Letters*, *38*, L16609. https://doi.org/10.1029/2011GL048538

Boudreau, B. P. (1994). Is burial velocity a master parameter for bioturbation? *Geochimica et Cosmochimica Acta*, *58*(4), 1243–1249. https://doi.org/10.1016/0016-7037(94)90378-6

Brennan, C. E., Bianucci, L., & Fennel, K. (2016). Sensitivity of northwest North Atlantic shelf circulation to surface and boundary forcing: A regional model assessment. *Atmosphere-Ocean*, *54*(3), 230–247.

Broecker, W. S., & Peng, T.-H. (1993). Evaluation of the ^{13}C constraint on the uptake of fossil fuel CO_2 by the ocean. *Global Biogeochemical Cycles*, *7*(3), 619–626.

Caesar, L., Rahmstorf, S., Robinson, A., Feulner, G., & Saba, V. (2018). Observed fingerprint of a weakening Atlantic Ocean overturning circulation. *Nature*, *556*(7700), 191.

Charbit, S., Rabouille, C., & Siani, G. (2002). Effects of benthic transport processes on abrupt climatic changes recorded in deep-sea sediments: A time-dependent modeling approach. *Journal of Geophysical Research*, *107*(C11), 3194. https://doi.org/10.1029/2000JC000575

Eide, M., Olsen, A., Ninnemann, U., & Eldevik, T. (2017a). A global estimate of the full oceanic ^{13}C Suess effect since the preindustrial. *Global Biogeochemical Cycles*, *31*, 1–23. https://doi.org/10.1002/2016GB005472

Eide, M., Olsen, A., Ninnemann, U., & Eldevik, T. (2017b). Suess effect since the preindustrial. *Global Biogeochemical Cycles*, *31*, 492–514. https://doi.org/10.1002/2016GB005472

Engstrom, D. R., & Swain, E. B. (1997). Recent declines in atmospheric mercury deposition in the upper Midwest. *Environmental Science and Technology*, *31*(4), 960–967. https://doi.org/10.1021/es9600892

Francey, R. J., Enting, I. G., Leuenberger, M., Langenfelds, R. L., Michel, E., & Steele, L. P. (1999). A 1000-year high precision record of d^{13}C in atmospheric CO. *Tellus*, *51B*(2), 170–193.

Ghaleb, B. (2009). Overview of the methods for the measurement and interpretation of short-lived radioisotopes and their limits. In *IOP conference series: Earth and environmental science* (Vol. 5, pp. 1–13). Bristol, England: IOP Publishing. https://doi.org/10.1088/1755-1307/5/1/012007

Gilbert, D., Sundby, B., Gobeil, C., Mucci, A., & Tremblay, G.-H. (2005). A seventy-two-year record of diminishing deep-water oxygen in the St. Lawrence estuary: The northwest Atlantic connection. *Limnology and Oceanography*, *50*(5), 1654–1666.

Gledhill, D. K., White, M. M., Salisbury, J., Thomas, H., Mlsna, I., Liebman, M., et al. (2015). Ocean and coastal acidification off New England and Nova Scotia. *Oceanography*, *28*(2), 182–197.

Graven, H., Allison, C. E., Etheridge, D. M., Hammer, S., Keeling, R. F., Levin, I., et al. (2017). Compiled records of carbon isotopes in atmospheric CO_2 for historical simulations in CMIP6. *Geoscientific Model Development*, *10*(12), 4405–4417.

Gruber, N., Keeling, C. D., Bacastow, R. B., Guenther, P. R., Lueker, T. J., Wahlen, M., et al. (1999). Spatiotemporal patterns of carbon-13 in the global abstract. A global ratio of dissolved inorganic carbon ocean water is governed by a balance between biological The most distinctive feature in the spatial distribution of 51 • C seen in our data is a max. *Global Biogeochemical Cycles*, *13*(2), 307–335. https://doi.org/10.1029/1999GB900019

Gruber, N., Clement, D., Carter, B. R., Feely, R. A., van Heuven, S., Hoppema, M., et al. (2019). The oceanic sink for anthropogenic CO_2 from 1994 to 2007. *Science*, *363*(6432), 1193–1199. https://doi.org/10.1126/science.aau5153

Gruber, N., & Keeling, C. D. (2001). An improved estimate of the isotopic air-sea disequilibrium of CO_2: Implications for the oceanic uptake of anthropogenic CO_2. *Geophysical Research Letters*, *28*(3), 555–558.

Heimann, M., & Maier-reimer, E. (1996). On the relations between the oceanic uptake of CO_2 and its carbon isotopes. *Global Biogeochemical Cycles*, *10*(1), 89–110.

Hemleben, C., & Bijma, J. (1994). Foraminiferal population dynamics and stable carbon isotopes. In R. Zahn (Ed.), *Carbon Cycling in the Glacial Ocean: Constraints on the Ocean's Role in Global Change* (pp. 145–166). Berlin, Heidelberg: Springer-Verlag.

Hesse, T., Wolf-Gladrow, D., Lohmann, G., Bijma, J., Mackensen, A., & Zeebe, R. E. (2014). Modelling δ^{13}C in benthic foraminifera: Insights from model sensitivity experiments. *Marine Micropaleontology*, *112*, 50–61.

Keeling, C. D. (1979). The Suess effect: ^{13}Carbon-^{14}carbon interrelations. *Environment International*, *2*(4–6), 229–300.

Keeling, C. D., Piper, S. C., Bacastow, M., Wahlen, M., Whorf, T. P., Heimann, M., & Meijer, H. A. (2001). *Exchanges of atmospheric CO2 and 13CO2 with the terrestrial biosphere and oceans from 1978 to 2000, Global aspects, SIO Reference Series* (Vol. 01–06). San Diego: Scripps Institute of Oceanography.

Keigwin, L. D., & Pilskaln, C. H. (2015). Sediment flux and recent paleoclimate in Jordan Basin, Gulf of Maine. *Continental Shelf Research*, *96*, 45–55. https://doi.org/10.1016/j.csr.2015.01.008

Keigwin, L. D., Sachs, J. P., & Rosenthal, Y. (2003). A 1600-year history of the Labrador Current off Nova Scotia. *Climate Dynamics*, *21*(1), 53–62.

King, A. L., & Howard, W. R. (2004). Planktonic foraminiferal D^{13}C records from Southern Ocean sediment traps: New estimates of the oceanic Suess effect. *Global Biogeochemical Cycles*, *18*, GB2007. https://doi.org/10.1029/2003GB002162

Körtzinger, A., Quay, P. D., & Sonnerup, R. E. (2003). Relationship between anthropogenic CO_2 and the ^{13}C suess effect in the North Atlantic Ocean. *Global Biogeochemical Cycles*, *17*(1), 1005. https://doi.org/10.1029/2001gb001427

Leipe, T., Moros, M., Kotilainen, A., Vallius, H., Kabel, K., Endler, M., & Kowalski, N. (2013). Mercury in Baltic Sea sediments—Natural background and anthropogenic impact. *Chemie Der Erde-Geochemistry*, *73*(3), 249–259.

Lynch-Stieglitz, J., Stocker, T. F., Broecker, W. S., & Fairbanks, R. G. (1995). The influence of air-sea exchange on the isotopic composition of oceanic carbon: Observations and modeling. *Global Biogeochemical Cycles*, *9*(4), 653–665.

McNeely, R., Dyke, A. S., & Southon, J. R. (2006). Canadian marine reservoir ages preliminary data assessment. Geological Survey of Canada.

McNeil, B. I., Matear, R. J., & Tilbrook, B. (2001). Does carbon 13 track anthropogenic CO_2 in the Southern Ocean? *Global Biogeochemical Cycles*, *15*(3), 597–613.

Mucci, A., Starr, M., Gilbert, D., & Sundby, B. (2011). Acidification of Lower St. *Lawrence Estuary Bottom Waters*, *49*(3), 206–218. https://doi.org/10.1080/07055900.2011.599265

Muggeo, V. M. R. (2003). Estimating regression models with unknown break-points. *Statistics in Medicine*, *22*(19), 3055–3071. https://doi.org/10.1002/sim.1545

Olsen, A., & Ninnemann, U. (2010). Large ^{13}C gradients in the preindustrial North Atlantic revealed. *Science*, *330*(6004), 658–659. https://doi.org/10.1126/science.1193769

Quay, P., Sonnerup, R., Stutsman, J., Maurer, J., Ko, A., Padin, X. A., & Robinson, C. (2007). Anthropogenic CO_2 accumulation rates in the North Atlantic Ocean from changes in the ^{13}C/^{12}C of dissolved inorganic carbon. *Global Biogeochemical Cycles*, *21*, GB1009. https://doi.org/10.1029/2006GB002761

Quay, P. D., Tilbrook, B., & Wong, C. S. (1992). Oceanic uptake of fossil fuel CO_2: Carbon-13 evidence. *Science*, *256*(5053), 74–79. https://doi.org/10.1126/science.256.5053.74

Rahmstorf, S., Box, J. E., Feulner, G., Mann, M. E., Robinson, A., Rutherford, S., & Schaffernicht, E. J. (2015). Exceptional twentieth-century slowdown in Atlantic Ocean overturning circulation. *Nature Climate Change*, *5*(5), 475.

Ravelo, A. C., & Hillaire-Marcel, C. (2007). The use of oxygen and carbon isotopes of foraminifera in paleoceanography. In C. Hillaire-Marcel & A. de Vernal (Eds.), *Proxies in the Late Cenozoic paleoceanography* (Vol. 1, pp. 735–764). Amsterdam, Oxford: Elsevier. https://doi.org/10.1016/S1572-5480(07)01023-8

Reimer, P. J., Bard, E., Bayliss, A., Beck, J. W., Blackwell, P. G., Ramsey, C. B., et al. (2013). IntCal13 and Marine13 radiocarbon age calibration curves 0–50,000 years cal BP. *Radiocarbon*, *55*(4), 1869–1887.

Rubino, M., Etheridge, D. M., Trudinger, C. M., Allison, C. E., Battle, M. O., Langenfelds, R. L., et al. (2013). A revised 1000 year atmospheric δ^{13}C-CO_2 record from Law Dome and South Pole, Antarctica. *Journal of Geophysical Research: Atmospheres*, *118*, 8482–8499. https://doi.org/10.1002/jgrd.50668

Sabine, C. L., Feely, R. A., Gruber, N., Key, R. M., Lee, K., Bullister, J. L., et al. (2004). The oceanic sink for anthropogenic CO_2. *Science*, *305*(5682), 367–371. https://doi.org/10.1126/science.1097403

Schöne, B. R., Wanamaker, A. D. Jr., Fiebig, J., Thébault, J., & Kreutz, K. (2011). Annually resolved δ^{13}C shell chronologies of long-lived bivalve mollusks (*Arctica islandica*) reveal oceanic carbon dynamics in the temperate North Atlantic during recent centuries. *Palaeogeography, Palaeoclimatology, Palaeoecology*, *302*(1–2), 31–42.

Sherwood, O. A., Lehmann, M. F., Schubert, C. J., Scott, D. B., & McCarthy, M. D. (2011). Nutrient regime shift in the western North Atlantic indicated by compound-specific δ^{15}N of deep-sea gorgonian corals. *Proceedings of the National Academy of Sciences of the United States of America*, *108*(3), 1011–1015. https://doi.org/10.1073/pnas.1004904108

Smith, J. N., & Schafer, C. T. (1999). Sedimentation, bioturbation, and Hg uptake in the sediments of the estuary and Gulf of St. Lawrence. *Limnology and Oceanography*, *44*(1), 207–219.

Sonnerup, R. E., Quay, D., Mcnichol, A. P., Bullister, L., & Anderson, L. (1999). Reconstructing the oceanic ^{13}C Suess effect. *Global Biogeochemical Cycles*, *13*(4), 857–872.

Sorgente, D., Frignani, M., Langone, L., & Ravaioli, M. (1999). Chronology of marine sediments: Interpretation of activity-depth profiles of ^{210}Pb and other radioactive tracers: PART I.

Spero, H. J., Bijma, J., Lea, D. W., & Bemis, B. E. (1997). Effect of seawater carbonate concentration on foraminiferal carbon and oxygen isotopes. *Nature*, *390*, 497–500.

Swart, P. K., Greer, L., Rosenheim, B. E., Moses, C. S., Waite, A. J., Winter, A., et al. (2010). The ^{13}C Suess effect in scleractinian corals mirror changes in the anthropogenic CO_2 inventory of the surface oceans. *Geophysical Research Letters*, *37*, L05604. https://doi.org/10.1029/2009GL041397

Tans, P. P., Berry, J. A., & Keeling, R. F. (1993). Oceanic ^{13}C/^{12}C observations: A new window on ocean CO_2 uptake. *Global Biogeochemical Cycles*, *7*(2), 353–368.

Thibodeau, B., Not, C., Zhu, J., Schmittner, A., Noone, D., Tabor, C., et al. (2018). Last century warming over the Canadian Atlantic shelves linked to weak Atlantic meridional overturning circulation. *Geophysical Research Letters*, *45*(22), 12,376–12,385. https://doi.org/10.1029/2018GL080083

Thomas, H., Friederike Prowe, A. E., van Heuven, S., Bozec, Y., de Baar, H. J. W., Schiettecatte, L. S., et al. (2007). Rapid decline of the CO_2 buffering capacity in the North Sea and implications for the North Atlantic Ocean. *Global Biogeochemical Cycles*, *21*, GB4001. https://doi.org/10.1029/2006GB002825

Thornalley, D. J. R., Oppo, D. W., Ortega, P., Robson, J. I., Brierley, C. M., Davis, R., et al. (2018). Anomalously weak Labrador Sea convection and Atlantic overturning during the past 150 years. *Nature*, *556*(7700), 227–230. https://doi.org/10.1038/s41586-018-0007-4